

# Hadronic Spectra from a Deformed AdS Background

---

Eduardo Folco Capossoli,<sup>a,b</sup> Miguel Angel Martín Contreras,<sup>c</sup> Danning Li,<sup>d</sup> Alfredo Vega,<sup>c</sup> Henrique Boschi-Filho<sup>a,1</sup>

<sup>a</sup>*Instituto de Física, Universidade Federal do Rio de Janeiro, 21.941-972 - Rio de Janeiro-RJ - Brazil*

<sup>b</sup>*Departamento de Física, Colégio Pedro II and Mestrado Profissional em Práticas da Educação Básica (MPPEB), 20.921-903 - Rio de Janeiro-RJ - Brazil*

<sup>c</sup>*Instituto de Física y Astronomía, Universidad de Valparaíso, A. Gran Bretaña 1111, Valparaíso, Chile*

<sup>d</sup>*Department of Physics and Siyuan Laboratory, Jinan University, Guangzhou 510632, China*

*E-mail:* [educapossoli@if.ufrj.br](mailto:educapossoli@if.ufrj.br), [miguelangel.martin@uv.cl](mailto:miguelangel.martin@uv.cl),  
[lidanning@jnu.edu.cn](mailto:lidanning@jnu.edu.cn), [alfredo.vega@uv.cl](mailto:alfredo.vega@uv.cl), [boschi@if.ufrj.br](mailto:boschi@if.ufrj.br)

**ABSTRACT:** Starting from a deformed  $AdS_5$  space due to the presence of a modified warp factor in the metric tensor of such space, we use the AdS/CFT correspondence within this model to calculate the spectra for even and odd glueballs, scalar and vector mesons, and baryons with different spins. For the glueball cases we derive their Regge trajectories and compare with the ones related to the pomeron and the odderon. In the case of the scalar and vector mesons and baryons the masses found here are compatible with the PDG. In particular for these hadrons we found Regge trajectories compatible with another holographic approach and also with the hadronic spectroscopy which present an universal Regge slope around  $1.1 \text{ GeV}^2$ .

---

<sup>1</sup>Corresponding author.

---

## Contents

<b>1</b>	<b>Introduction</b>	<b>1</b>
<b>2</b>	<b>The Softwall Model and the Deformed AdS Set Up</b>	<b>2</b>
<b>3</b>	<b>Hadronic Spectra for glueballs states</b>	<b>3</b>
3.1	Results for even and odd spin glueball spectra	4
<b>4</b>	<b>Hadronic Spectra for scalar mesons</b>	<b>7</b>
4.1	Results for scalar mesons spectra	7
<b>5</b>	<b>Hadronic Spectra for vector mesons</b>	<b>10</b>
5.1	Results for vector mesons spectra	11
<b>6</b>	<b>Hadronic spectra for baryons</b>	<b>14</b>
6.1	Results for spin 1/2 baryons spectra	16
6.2	Results for higher spin baryons spectra	19
<b>7</b>	<b>Summary and conclusions</b>	<b>21</b>

---

## 1 Introduction

Quantum Chromodynamics (QCD) is a non-abelian quantum field theory and it is the appropriate theory to deal with the strong interactions. Although its enormous success in high energies, it is very difficult to use QCD to investigate processes that occur at low energies (IR regions) because of the failure of the perturbative approach in this case. This peculiar feature of the QCD is related to the fact that it is a confining theory in the IR, implying that only bound states of quarks or gluons are observed.

Hadronic spectroscopy still remains an amazing field to apply new approaches in order to extract information about the hadronic properties once we can compare our results with the experimental data. Many works were done in order to study hadronic spectroscopy using AdS/CFT correspondence.

Among several techniques to handle it there is one that emerged in 1997 proposed by Juan Maldacena called Anti de Sitter/Conformal Field Theory or AdS/CFT correspondence [1–5]. This correspondence is very useful, once it teaches us how to relate a weak coupling theory represented, in this case, by a superstring theory in a ten dimensional curved space, named  $AdS_5 \times S^5$  with a strong coupling theory, in this case, a super conformal Yang-Mills theory, with extended supersymmetry  $\mathcal{N} = 4$ , symmetry group  $SU(N \rightarrow \infty)$  in a flat four dimensional Minkowski space.

Even so, one cannot use directly the AdS/CFT correspondence to reproduce QCD, since it is not a conformal theory.

Some proposals appeared to break the conformal invariance and build effective theories known as AdS/QCD models, as for example, the hardwall model. In this model the conformal symmetry is broken via an introduction of a hard IR cutoff at a certain value  $z_{max}$  of the holographic coordinate  $z$  and just considering a slice of  $AdS_5$  space in the interval  $[0, z_{max}]$  [6–8]. For the achievement related the hadronic spectroscopy within the hardwall model one can see, for instance [9–14].

Another example of breaking the conformal invariance is given by the softwall model. In this model one uses a soft IR cutoff via an introduction of a dilaton field in the action. Such approach was proposed in [15] in order to study the mesonic spectroscopy. Usually one refers to this model as the original softwall model. Soon after, other modifications of this model to deal with hadronic spectroscopy were considered, for instance, in [16–24]. Going further in some modification the Refs.[25–29] instead of the introduction of a dilation in the action, a modified warp factor in the AdS metric was considered. Particularly, in [25] such modification was proposed to study hadronic spectroscopy, in [26–28] the modification was used to discuss the quark-antiquark potential and in [29] to deal with scalar and tensor glueballs.

Here, inspired in [25, 26], we will consider a modified warp factor in the  $AdS_5$  metric instead of introducing a dilaton field in the action. In this sense, in our set up we are considering a deformed AdS background. Then, we compute the hadronic spectra for different particles within this model.

This work is organized as follows. In section 2 we will present a brief review of the original softwall model and our deformed AdS background. In section 3 we apply our model to the even and odd spin glueball states. In section 4, we study the case of scalar mesons obtaining their spectra. In section 5 we will calculate the hadronic spectra for the vector mesons and in section 6 for the baryonic case with spins  $1/2$ ,  $3/2$  and  $5/2$ . For those particles we also obtain the corresponding Regge trajectories. In particular, for the glueballs we derive the Regge trajectories related to the pomeron and the odderon. Finally in section 7 we will present our conclusions and last comments.

## 2 The Softwall Model and the Deformed AdS Set Up

There are, at least, two interesting reasons for the emergence of the Softwall model. The first one is related to the introduction of the soft IR cutoff instead a hard cutoff like the hardwall model, since this approach seems to be more natural than the other one. The second reason lies in the fact that softwall model really provides linear Regge trajectories, which was already a known behavior since the beginning of hadronic spectroscopy, so that

$$J(m) \approx \alpha' m^2 + \alpha_0, \quad (2.1)$$

where  $J$  is the total angular momenta,  $m$  represents the hadronic masses, while  $\alpha'$  (Regge slope) and  $\alpha_0$  are constants. In this sense, one also can see a relationship between radial

excitation  $n$  and its squared hadron masses, given by:

$$m^2 \approx \beta' n + \beta_0, \quad (2.2)$$

with  $\beta'$  and  $\beta_0$  constants.

In the original formulation of the original softwall model, the action of the fields, up to some constant, is described by:

$$S = \int d^5x \sqrt{-g} e^{-\Phi(z)} \mathcal{L}, \quad (2.3)$$

where  $\Phi(z)$  is the dilaton field, usually given by  $\Phi(z) = kz^2$ , with  $|k| \sim \Lambda_{QCD}^2$ , and  $\mathcal{L}$  is the Lagrangian density.

The main difference between the original softwall and the present work is that here we modify the  $AdS_5$  metric tensor using an exponential warp factor for all glueballs and hadrons. One should note that in Ref. [25] the authors have used different warp factor profiles, usually logarithm ones, for each hadronic sector.

As we are using the same warp factor profile in the AdS space for all glueballs and hadrons we are calling this approach here, as mentioned before, as a deformed  $AdS_5$  background. Then, we write the deformed  $AdS_5$  metric as:

$$ds^2 = g_{mn} dx^m dx^n = \frac{R^2}{z^2} e^{kz^2} (dz^2 + \eta_{\mu\nu} dx^\mu dx^\nu) = e^{2A(z)} (dz^2 + \eta_{\mu\nu} dx^\mu dx^\nu), \quad (2.4)$$

where  $R$  is the usual AdS radius (from now on we take  $R = 1$  throughout this text),  $\eta_{\mu\nu}$  is the flat Minkowski space metric tensor in four dimensions with signature  $(-, +, +, +)$ ,  $z$  is the holographic coordinate and  $x^m = (z, x^\mu)$  for  $\mu = 0, \dots, 3$ . The warp factor  $A(z)$  in (2.4) can be read as:

$$A(z) = -\log(z) + \frac{kz^2}{2}. \quad (2.5)$$

Now, in our model the action for the fields is simply:

$$S = \int d^5x \sqrt{-g} \mathcal{L}, \quad (2.6)$$

where  $g$  is the determinant of the five-dimensional metric tensor presented in (2.4).

### 3 Hadronic Spectra for glueballs states

Let us start this section quoting Fritzsche and Gell-Mann as pointed out in Refs [30, 31]. So that, “If the quark-gluon field theory indeed yields a correct description of strong interactions, there must exist glue states in the hadron spectrum”. This sentence does really reveals the importance of those “glue states” nowadays called glueballs. Glueballs are colorless bound states of gluons predicted by QCD but not detected so far.

Glueballs are characterized by  $J^{PC}$  where  $J$  (even or odd) is the total angular momentum,  $P$  is the  $P$ -parity (spatial inversion) and  $C$  is the  $C$ -parity (charge conjugation) eigenvalues. For the glueballs case  $P = (-1)^L$  and  $C = (-1)^{L+S}$ .

Many experimental efforts in order to search for glueballs were done as one can see for instance in [32–35]. Within the theoretical and non-holographic approaches, one can see for instance in [36–41]. On the other hand, for the holographic approach, one can see [42–51].

Here in this work based on a deformed AdS space, as discussed in the previous section, we will compute the masses of the even spin glueballs with  $P = C = +1$  and odd spin glueballs with  $P = C = -1$ . Even spin glueballs with  $P = C = +1$  are specially interesting since in the Chew-Frautschi plane, their states lie on the Pomeron Regge trajectory. On the other hand, odd spin glueballs with  $P = C = -1$  lie on the odderon Regge trajectory.

After this quick digression about glueballs we will start our calculation using the standard action for a massive scalar field  $X$  in  $5D$  space, given by:

$$S = \int d^5x \sqrt{-g} [g^{mn} \partial_m X \partial_n X + M_5^2 X^2]. \quad (3.1)$$

From the action (3.1) one can find the following equations of motion, so that:

$$\partial_m [\sqrt{-g} g^{mn} \partial_n X] - \sqrt{-g} M_5^2 X = 0, \quad (3.2)$$

where  $g^{mn} = e^{-2A(z)} \eta^{\mu\nu}$ .

The equations in (3.2) can be written as:

$$\partial_m [e^{3A(z)} \eta^{mn} \partial_n X] - e^{5A(z)} M_5^2 X = 0, \quad (3.3)$$

with the warp factor  $A(z)$  given in (2.5).

Now, defining  $B(z) = -3A(z)$ , one has:

$$\partial_m [e^{-B(z)} \eta^{mn} \partial_n X] - e^{\frac{-5B(z)}{3}} M_5^2 X = 0. \quad (3.4)$$

Next, we use a plane wave ansatz with amplitude just depending on the  $z$  coordinate and propagating in the transverse coordinates  $x^\mu$  with momentum  $q_\mu$ ,

$$X(z, x^\mu) = v(z) e^{iq_\mu x^\mu}. \quad (3.5)$$

After some algebraic manipulation and defining  $v(z) = \psi(z) e^{\frac{B(z)}{2}}$  one has a ‘‘Schrödinger-like’’ equation:

$$-\psi''(z) + \left[ \frac{B'^2(z)}{4} - \frac{B''(z)}{2} + e^{\frac{-2B(z)}{3}} M_5^2 \right] \psi(z) = -q^2 \psi(z), \quad (3.6)$$

with  $B(z) = -3A(z)$  and  $E = -q^2$  are the eigenenergies.

### 3.1 Results for even and odd spin glueball spectra

In order to compute the glueball masses one has to solve numerically the Eq.(3.6). To do this, firstly from the AdS/CFT dictionary we know how to relate the masses of supergravity fields in AdS space ( $M_5$ ) with the scaling dimensions of an operator in the boundary theory ( $\Delta$ ), so that:

$$M_5^2 = (\Delta - p)(\Delta + p - 4), \quad (3.7)$$

	Even Glueball States $J^{PC}$					
	$0^{++}$	$2^{++}$	$4^{++}$	$6^{++}$	$8^{++}$	$10^{++}$
Masses	0.76	2.08	3.17	4.22	5.26	6.30

**Table 1.** Even glueball masses expressed in GeV from Eq. (3.11) with the warp factor constant  $k$  given by  $k_{\text{gbe}} = 0.31^2 \text{ GeV}^2$ .

where  $p$  is the index of a  $p$ -form. For the case of the scalar glueball  $0^{++}$  one has  $p = 0$ . Besides the scalar glueball is dual to the fields with  $M_5 = 0$ , then its conformal dimension is  $\Delta = 4$ .

Secondly is also known that the scalar glueball state is represented on the boundary theory by the operator  $\mathcal{O}_4$ , given by:

$$\mathcal{O}_4 = \text{Tr} (F^2) = \text{Tr} (F^{\mu\nu} F_{\mu\nu}). \quad (3.8)$$

In order to raise the total angular momentum  $J$  we will follow [11] by inserting symmetrised covariant derivatives in a given operator with spin  $S$ , such that, the total angular momentum after the insertion is now  $S + J$ . In the particular case of the operator  $\mathcal{O}_4 = \text{Tr} F^2$ , one gets:

$$\mathcal{O}_{4+J} = \text{Tr} (F D_{\{\mu_1 \dots \mu_J\}} F), \quad (3.9)$$

with conformal dimension  $\Delta = 4 + J$ . For  $J = 0$  we recover  $\Delta = 4$ .

So, for even spin glueball states after the insertion of symmetrised covariant derivatives, one has:

$$M_5^2 = J(J + 4); \quad (\text{even } J). \quad (3.10)$$

Now one can write Eq.(3.6) as:

$$-\psi''(z) + \left[ \frac{B'^2(z)}{4} - \frac{B''(z)}{2} + e^{\frac{-2B(z)}{3}} J(J + 4) \right] \psi(z) = -q^2 \psi(z). \quad (3.11)$$

Solving Eq.(3.11), for even glueball states, one gets the four dimensional masses presented in Table 1.

From Table 1 we plotted a Chew-Frautschi plane here represented as  $m^2 \times J$ , where  $J$  is total angular momentum and  $m^2$  is the squared even glueball mass represented by the dots in figure 1. From a standard linear regression method we obtain the equation

$$J(m^2) \approx (0.25 \pm 0.02)m^2 + (0.88 \pm 0.51), \quad (3.12)$$

representing an approximate linear Regge trajectory associated with the pomeron in agreement with [52, 53].

On the other hand, for odd glueball states, the operator  $\mathcal{O}_6$  that describes the glueball state  $1^{--}$  is given by:

$$\mathcal{O}_6 = \text{Sym Tr} (\tilde{F}_{\mu\nu} F^2), \quad (3.13)$$

which has conformal dimension  $\Delta = 6$  and after the insertion of symmetrised covariant derivatives one gets:

$$\mathcal{O}_{6+J} = \text{Sym Tr} (\tilde{F}_{\mu\nu} F D_{\{\mu_1 \dots \mu_J\}} F), \quad (3.14)$$

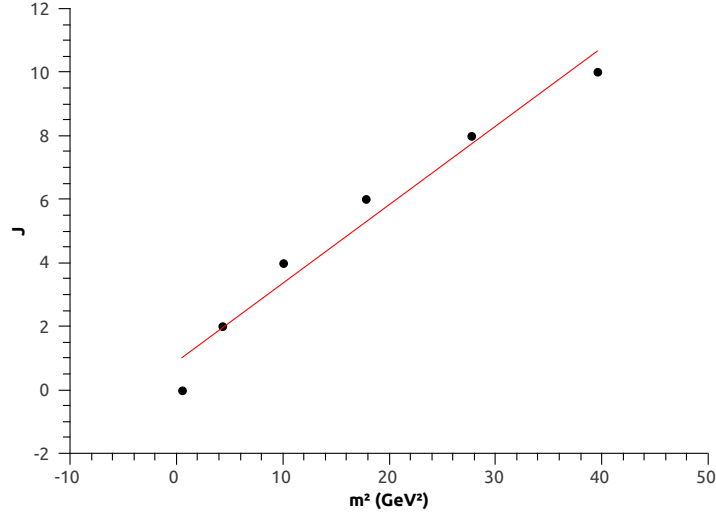


**Figure 1.** Approximate linear Regge trajectory associated with the pomeron from Eq. (3.12). The dots correspond to the masses found in Table 1 for even glueball states within the deformed  $AdS_5$  space approach .

	Odd Glueball states $J^{PC}$					
	$1^{--}$	$3^{--}$	$5^{--}$	$7^{--}$	$9^{--}$	$11^{--}$
Masses	2.63	3.70	4.74	5.78	6.81	7.84

**Table 2.** Odd spin glueball masses expressed in GeV from Eq.(3.16) with the warp factor constant  $k$  given by  $k_{\text{gbo}} = 0.31^2 \text{ GeV}^2$ .

with  $\Delta = 6 + J$ . Now one has:

$$M_5^2 = (J + 6)(J + 2); \quad (\text{odd } J), \quad (3.15)$$

and one can rewrite Eq.(3.6) as:

$$-\psi''(z) + \left[ \frac{B'^2(z)}{4} - \frac{B''(z)}{2} + e^{\frac{-2B(z)}{3}}(J + 6)(J + 2) \right] \psi(z) = -q^2 \psi(z). \quad (3.16)$$

Solving Eq.(3.16) for odd glueball states, one gets the four dimensional masses presented in Table 2.

From Table 2 we plotted a Chew-Frautschi plane  $m^2 \times J$  in figure 2 for odd spin glueballs. From a standard linear regression method we obtain the equation

$$J(m^2) \approx (0.18 \pm 0.01)m^2 + (0.47 \pm 0.45), \quad (3.17)$$

in agreement with [54], within the nonrelativistic constituent model.

One should note that the value for the constant  $k$  in the warp factor  $A(z)$  for even spin glueball represented by  $k_{\text{gbe}}$  and for odd spin glueball represented by  $k_{\text{gbo}}$  have the same numerical value  $k_{\text{gbe}} = k_{\text{gbo}} = 0.31^2 \text{ GeV}^2$ .

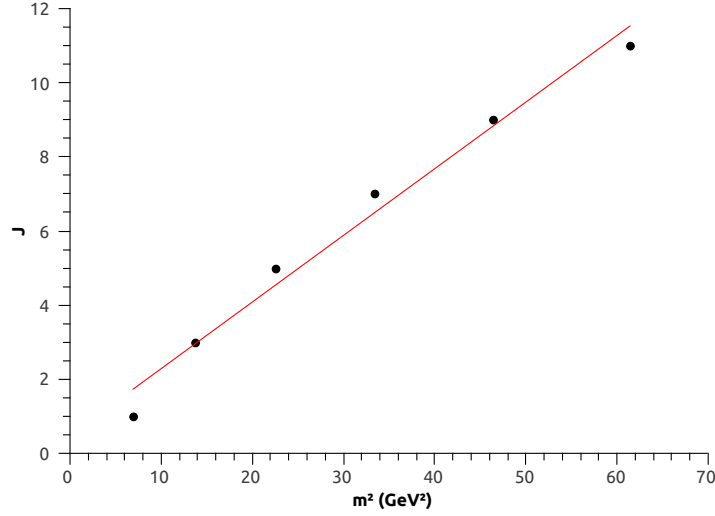


**Figure 2.** Approximate linear Regge trajectory associated with the odderon from Eq. (3.17). The dots correspond to the masses found in Table 2 within the deformed  $AdS_5$  space approach for odd spin glueballs.

## 4 Hadronic Spectra for scalar mesons

Mesons are a bound states between a quark and an antiquark which can be represented by a spin singlet with total spin  $S = 0$  or a spin triplet with total spin  $S = 1$ . Besides one has to take into account the coupling between  $S$  and the orbital angular momentum  $L$  producing a total angular momentum  $J = L$  in the case of the singlet state, and  $J = L - 1, L, L + 1$  in the case of the triplet state.

From mesonic spectroscopy [55], mesons are characterized by  $I^G(J^{PC})$ , where  $I$  is the isospin,  $G$  is the  $G$ -parity defined  $G = (-1)^I = \pm 1$ ,  $P$  is the  $P$ -parity defined for mesons as  $P = (-1)^{L+1}$ . Finally,  $C$  is the  $C$ -parity defined as  $C = (-1)^{L+S}$ . On the boundary theory scalar mesons are represented by the operator:

$$\mathcal{O}_{SM} = \bar{q} D_{\{J_1 \dots J_m\}} q \quad \text{with} \quad \sum_{i=1}^m J_i = J, \quad (4.1)$$

where  $J$  is the total angular momentum.

In this section we are interested in light scalar mesons meaning  $J = 0$  and unflavored ( $S = C = B = 0$ ).

Within the holographic approach the description of the scalar glueball ( $gg$ ) and the scalar meson ( $q\bar{q}$ ) is the same, but the main difference is given by the bulk mass, defining the hadron identity. Then, to study the scalar meson one has to start from action for a massive scalar field (3.1) which will leads us to the “Schrödinger-like” equation (3.6).

### 4.1 Results for scalar mesons spectra

Using again the relationship  $M_5^2 = (\Delta - p)(\Delta + p - 4)$ , now identifying  $M_5$  with the scalar meson bulk mass, the index of the  $p$ -form with the total angular momentum ( $p = J = 0$ )



	Scalar Meson $f_0$ ( $0^+(0^{++})$ )			
	$f_0$ meson	$M_{\text{exp}}$ GeV [56]	$M_{\text{th}}$ GeV	$\%M$
$n = 1$	$f_0(980)$	$0.990 \pm 0.02$	1.089	9.97
$n = 2$	$f_0(1370)$	1.2 to 1.5	1.343	0.54
$n = 3$	$f_0(1500)$	$1.504 \pm 0.006$	1.562	3.87
$n = 4$	$f_0(1710)$	$1.723^{+0.006}_{-0.005}$	1.757	1.96
$n = 5$	$f_0(2020)$	$1.992 \pm 0.016$	1.933	2.96
$n = 6$	$f_0(2100)$	$2.101 \pm 0.007$	2.095	0.27
$n = 7$	$f_0(2200)$	$2.189 \pm 0.013$	2.246	2.61
$n = 8$	$f_0(2330)$	$2.337 \pm 0.014$	2.388	2.17

**Table 3.** Masses of light unflavored scalar meson  $f_0$  ( $S = C = B = 0$ ). The column  $n = 1, 2, 3, \dots$  represents the holographic radial excitation of the scalar mesons. The ground state here is represented by  $n = 1$ . The column  $M_{\text{exp}}$  represents the experimental data coming from PDG [56]. The column  $M_{\text{th}}$  represents the masses obtained within the deformed  $AdS_5$  space approach using Eq.(4.2) with  $k_{\text{sm}} = -0.332^2 \text{ GeV}^2$ . The column  $\%M$  represents the error of  $M_{\text{th}}$  with respect to  $M_{\text{exp}}$ , accordingly to Eq. (4.3).

for the scalar meson and  $\Delta$  with their conformal dimension, which is  $\Delta = 3$  since each quark contributes with  $3/2$ . Finally one can rewrite Eq.(3.6) with  $M_\xi^2 = -3$  as:

$$-\psi''(z) + \left[ \frac{B'^2(z)}{4} - \frac{B''(z)}{2} - 3 e^{\frac{-2B(z)}{3}} \right] \psi(z) = -q^2 \psi(z), \quad (4.2)$$

where  $B(z) = -3A(z)$ . Solving numerically (4.2) with the warp factor constant  $k$  now identified with  $k_{\text{sm}} = -0.332^2 \text{ GeV}^2$  we get the masses compatible with the family of the scalar meson  $f_0$ , with  $I^G J^{PC} = 0^+(0^{++})$ , as can be seen in table 3. Note that the error presented in last column of Table 3 ( $\%M$ ) is the error defined by:

$$\%M = \sqrt{\left( \frac{\delta O_i}{O_i} \right)^2} \times 100, \quad (4.3)$$

where  $\delta O_i$  are the deviations between the data ( $M_{\text{exp}}$ ) and the model prediction ( $M_{\text{th}}$ ). Throughout the text, in the cases where the experimental data comes as an interval, as the  $f_0(1370)$  state, we use the the average value of the interval to evaluate the deviations. We also compute the total r.m.s error defined by:

$$\delta_{rms} = \sqrt{\frac{1}{N - N_p} \sum_{i=1}^N \left( \frac{\delta O_i}{O_i} \right)^2} \times 100, \quad (4.4)$$

where  $N$  and  $N_p$  are the number of measurements and parameters, respectively. From (4.4) one finds that  $\delta_{rms} = 3.77\%$  for table 3.

From Table 3 we plotted a Chew-Frautschi plane here represented as  $n \times m^2$ , where  $n$  is holographic radial excitation and  $m^2$  is the squared scalar meson mass represented by the dots (our model) or squares (PDG) in figure 3. From a standard linear regression

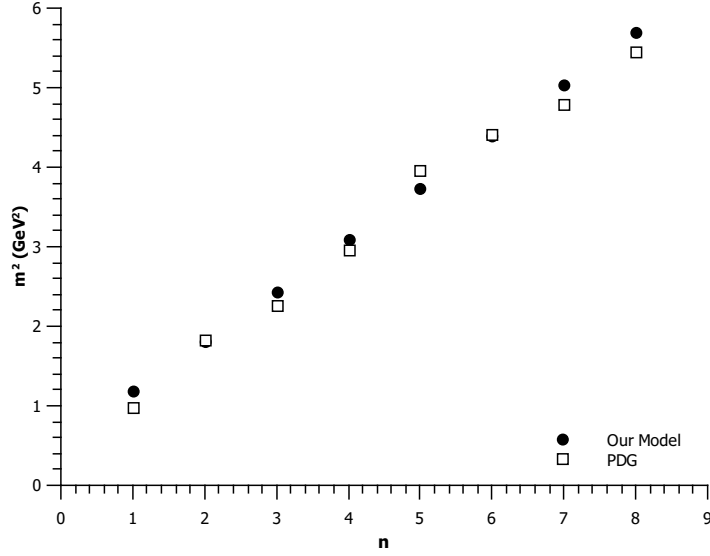


**Figure 3.** Scalar meson  $f_0$  family squared masses as a function of their holographic radial excitation  $n$  obtained within the deformed  $AdS_5$  space approach (dots) and coming from PDG (squares), as presented in Table 3.

method we obtain the experimental and theoretical Regge trajectories for the scalar meson  $f_0$  family, so that:

$$m_{Exp}^2 = (0.639 \pm 0.027) n + (0.458 \pm 0.135), \quad (4.5)$$

$$m_{th}^2 = (0.647 \pm 0.002) n + (0.513 \pm 0.011). \quad (4.6)$$

The authors in Refs. [57, 58] within a holographic softwall model also computed the masses for  $f_0$  meson family and derived its Regge trajectory slightly different from Eq. (4.6). This can be possible explained since the data selection scenarios in these references are different from the current work. In these references it was included the scalar meson  $f_0(500)$ , and possibly, this might cause the slightly difference of the slope and the intercept if compared to ours.

In order to connect our results with the mesonic spectroscopy data [55, 59–61] we can split the isoscalar states  $f_0$  into two sets. The first set, namely set 1, is related to the  $n\bar{n} = (u\bar{u} + d\bar{d})/\sqrt{2}$  states which is represented by  $f_0(980)$ ,  $f_0(1500)$ ,  $f_0(2020)$  and  $f_0(2200)$ . The second set, namely set 2, is related to  $s\bar{s}$  states also called  $f'_0$ , which is represented by  $f_0(1370)$ ,  $f_0(1710)$ ,  $f_0(2100)$  and  $f_0(2330)$ .

Using the states that belong to set 1 we can plot a Chew-Frautschi plane here represented as  $n_r \times m^2$ , where  $n_r$  is spectroscopy radial excitation and  $m^2$  is the squared scalar meson mass represented by the dots (our model) or squares (PDG) in figure 4. From a standard linear regression method we obtain the experimental and theoretical Regge trajectories for set 1, given by:

$$m_{Exp}^2 = (1.314 \pm 0.017) n_r - (0.285 \pm 0.332), \quad (4.7)$$

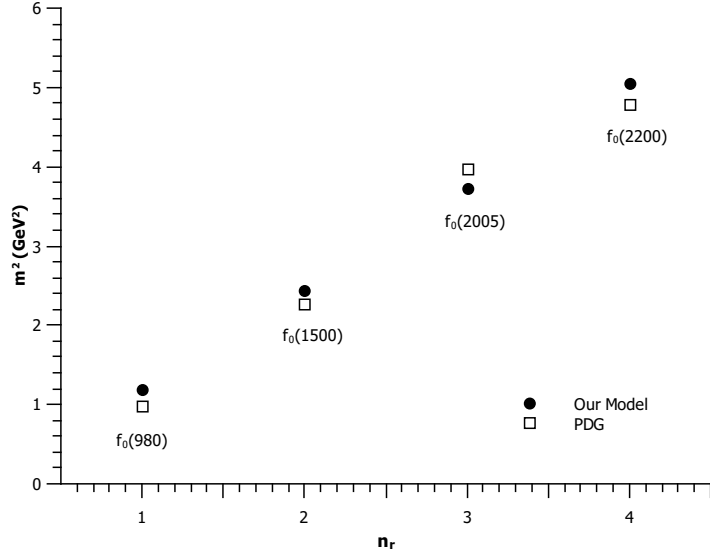


**Figure 4.** Scalar meson  $f_0$  [ $n\bar{n} = (u\bar{u} + d\bar{d})/\sqrt{2}$ ] states belonging to set 1 (see the text) squared masses as a function of their spectroscopy radial excitation  $n_r$  obtained within the deformed  $AdS_5$  space approach (dots) and coming from PDG (squares).

$$m_{th}^2 = (1.288 \pm 0.009) n_r - (0.117 \pm 0.024). \quad (4.8)$$

Doing the same for the states belonging to set 2 we plot the figure 5 and obtain the experimental and theoretical Regge trajectories, given by:

$$m_{Exp}^2 = (1.236 \pm 0.052) n_r - (0.576 \pm 0.142), \quad (4.9)$$

$$m_{th}^2 = (1.300 \pm 0.005) n_r - (0.496 \pm 0.012). \quad (4.10)$$

Note that the Regge trajectories for the scalar mesons belonging to the set 1 and 2 coming from our model, represented by Eqs. (4.8) and (4.10), present Regge slopes ranged within the  $1.25 \pm 0.15 \text{ GeV}^2$  which is close to the universal value  $1.1 \text{ GeV}^2$  [59, 62].

## 5 Hadronic Spectra for vector mesons

Vector mesons have the same internal structure ( $q\bar{q}$ ) as the scalar mesons but now with total angular momentum  $J = 1$ . They are represented on the boundary theory by the operator:

$$\mathcal{O}_{VM} = \bar{q} \gamma^\mu D_{\{J_1 \dots J_m\}} q \quad \text{with} \quad \sum_{i=1} J_i = J. \quad (5.1)$$

In the holographic description vector mesons are dual to the massive vector field in the  $AdS_5$ , then one needs the action for massive vector field, given by:

$$S = -\frac{1}{2} \int d^5x \sqrt{-g} \left[ \frac{1}{2} g^{pm} g^{qn} F_{mn} F_{pq} + M_5^2 g^{pm} A_p A_m \right], \quad (5.2)$$

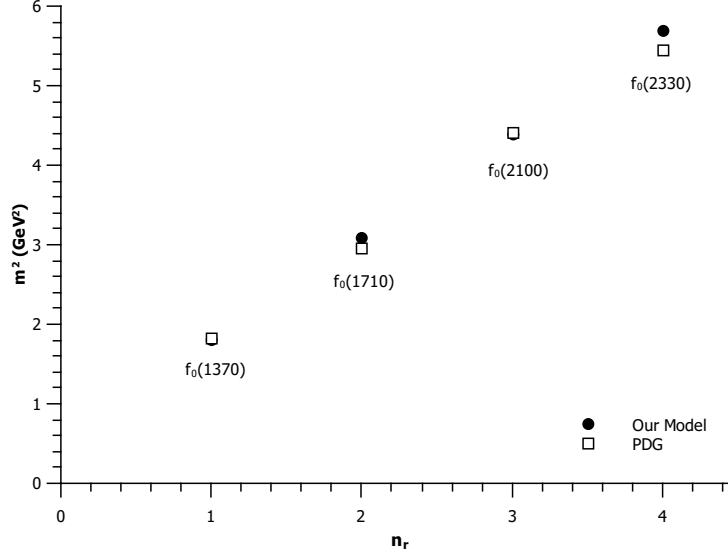


**Figure 5.** Scalar meson  $f_0[s\bar{s}]$  states belonging to set 2 (see the text) squared masses as a function of their spectroscopy radial excitation  $n_r$  obtained within the deformed  $AdS_5$  space approach (dots) and coming from PDG (squares).

where the vector field stress tensor is defined as  $F_{mn} = \partial_m A_n - \partial_n A_m$ .

The equations of motion are achieved by  $\delta S / \delta A_n = 0$ , so that:

$$\partial_z [e^{-B(z)} F_{zn} \eta^{nq}] + \partial_\mu [e^{-B(z)} \eta^{m\mu} F_{mn} \eta^{nq}] - e^{-3B(z)} M_5^2 A_n \eta^{nq} = 0, \quad (5.3)$$

where  $B(z) = -A(z)$ .

Considering a plane wave ansatz with amplitude just depending on the  $z$  coordinate and propagating in the transverse coordinates  $x^\mu$  with momentum  $q_\mu$ , we have

$$A_\nu(z, x^\mu) = v(z) e^{iq_\mu x^\mu} \epsilon_\nu, \quad (5.4)$$

assuming  $A_z = 0$  and  $\epsilon^\nu \epsilon_\nu = \eta^{\nu\lambda} \epsilon_\nu \epsilon_\lambda = 1$  is the unitary 4-vector defined in the transverse space to  $z$  coordinate, with components  $\epsilon_\nu = 1/2(1, 1, 1, 1)$ . We use the fact  $\partial_\mu A^\mu = 0$  that implies  $q^\mu \epsilon_\mu = \eta^{\mu\lambda} q_\mu \epsilon_\lambda = q \cdot \epsilon = 0$  ensuring that the field can be written as a plane wave. Note that  $F_{zn} = \partial_z A_n$  and  $\eta^{m\mu} \partial_\mu F_{mn} = -q^2 A_n$ . After some algebraic manipulation and defining  $v(z) = \psi(z) e^{\frac{B(z)}{2}}$ , one has the ‘Schrödinger-like’ equation, given by:

$$-\psi''(z) + \left[ \frac{B'^2(z)}{4} - \frac{B''(z)}{2} + e^{-2B(z)} M_5^2 \right] \psi(z) = -q^2 \psi(z), \quad (5.5)$$

where  $E = -q^2$  are the eigenenergies.

### 5.1 Results for vector mesons spectra

Here in this subsection we are going consider the case  $J = 1$ . Then recalling  $M_5^2 = (\Delta - p)(\Delta + p - 4)$ , now identifying  $M_5$  as the vector meson bulk mass, the index of  $p$ -form

	Vector Meson $\rho(1^+(1^{--}))$			
	$\rho$ meson	$M_{\text{exp}}$ GeV [56]	$M_{\text{th}}$ GeV	$\%M$
$n = 1$	$\rho(770)$	$0.77526 \pm 0.00025$	0.868327	12.0422
$n = 2$	$\rho(1450)$	$1.465 \pm 0.025$	1.228	16.1775
$n = 3$	$\rho(1570)$	$1.570 \pm 0.070$	1.50399	4.20467
$n = 4$	$\rho(1700)$	$1.720 \pm 0.020$	1.73665	0.968271
$n = 5$	$\rho(1900)$	$1.909 \pm 0.042$	1.94164	1.70972
$n = 6$	$\rho(2150)$	$2.155 \pm 0.021$	2.12696	1.30123

**Table 4.** Masses of light unflavored vector meson  $\rho$  ( $S = C = B = 0$ ). The column  $n = 1, 2, 3, \dots$  represents the holographic radial excitation of the vector mesons. The ground state here is represented by  $n = 1$ . The column  $M_{\text{exp}}$  represents the experimental data coming from PDG [56]. The column  $M_{\text{th}}$  represents the masses obtained within the deformed  $AdS_5$  space approach and using Eq.(5.6) with  $k_{\text{vm}} = -0.613^2$  GeV<sup>2</sup>. The column  $\%M$  represents the error of  $M_{\text{th}}$  with respect to  $M_{\text{exp}}$ , accordingly to Eq. (4.3).

as total angular momentum ( $p = J = 1$ ) for the vector meson and  $\Delta$  as the conformal dimension, which is  $\Delta = 3$  since each quark contributes with  $3/2$ . Finally one can rewrite Eq.(5.5) as:

$$-\psi''(z) + \left[ \frac{B'^2(z)}{4} - \frac{B''(z)}{2} \right] \psi(z) = -q^2 \psi(z), \quad (5.6)$$

with  $B(z) = -A(z)$  and  $M_5^2 = 0$  for vector mesons.

Solving numerically (5.6) with the warp factor constant  $k$  now given by  $k_{\text{vm}} = -0.613^2$  GeV<sup>2</sup> we get the masses compatibles with the family of vector meson  $\rho$ , with  $I^G J^{PC} = 1^+(1^{--})$ , as can be seen in table 4. Note that the error presented in last column of Table 4 ( $\%M$ ) was defined in Eq.(4.3). We also compute the total r.m.s error defined by Eq. (4.4). For table 4 one finds  $\delta_{rms} = 7.87\%$ .

From Table 4 we plotted a Chew-Frautschi plane here represented as  $n \times m^2$ , where  $n$  is the holographic radial excitation and  $m^2$  is the squared vector meson mass represented by the dots (our model) or squares (PDG) in figure 6. From a standard linear regression method we obtain the experimental and theoretical Regge trajectories for vector meson  $\rho$ , so that:

$$m_{Exp}^2 = (0.720 \pm 0.076) n - (0.223 \pm 0.302), \quad (5.7)$$

$$m_{th}^2 = (0.754 \pm 8 \times 10^{-7}) n. \quad (5.8)$$

We did not include the intercept in Eq. (5.8) because its value is very close to zero ( $\approx 10^{-18}$ ). Note also that in Eq. (5.8) the uncertainty in the slope is very small indicating that this fit is practically a straight line.

The authors in the Refs. [57, 58] within their holographic softwall model also computed the masses for  $\rho$  meson family and derived its Regge trajectory obtaining approximately the same value for the slope and intercept (considering the uncertainties) in relation to our result, Eq. (5.8). It is worthy to mention that the data selection scenarios in those references are different from the current work. In those references it was included the vector

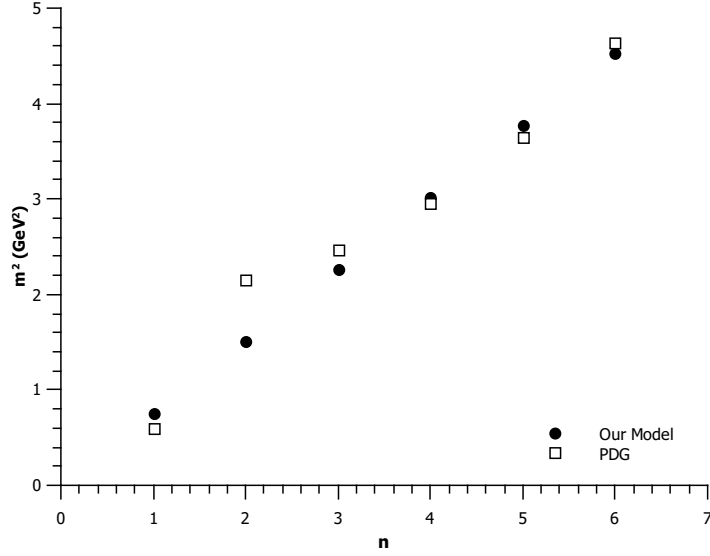


**Figure 6.** Vector meson  $\rho$  family squared masses as a function of their holographic radial excitation obtained within the deformed  $AdS_5$  space approach (dots) and coming from PDG (squares), as presented in Table 4.

meson  $\rho(1282)$  as the first radial excited state and it was excluded the vector meson  $\rho(1570)$  which the authors argue that it may be an OZI violating decay of the  $\rho(1700)$ . If we assume the existence of the  $\rho(1282)$  as the first radial excitation ( $n = 2$ ) of the  $\rho$  meson family, then the corresponding percentage error  $\%M$  in Table 4 would be smaller as well as the  $\delta_{rms}$  error.

As done for scalar mesons, one can resort to the mesonic spectroscopy data [55, 59–61] and note that all vector mesons listed in Table 4 are not in the same spectroscopic state, meaning that only  $\rho(770)$ ,  $\rho(1450)$ ,  $\rho(1900)$  and  $\rho(2150)$  belong to the  $S$ -wave represented by  $1^3S_1$ ,  $2^3S_1$ ,  $3^3S_1$  and  $4^3S_1$ , respectively. Here we have used the spectroscopic notation, such as,  $n_r^{2S+1}L_J$ , where  $n_r$  is the spectroscopy radial excitation. Using these states one can plot in a Chew-Frautschi plane here represented as  $n_r \times m^2$ , where  $n_r$  is the spectroscopy radial excitation and  $m^2$  is the squared vector meson mass represented by the dots (our model) or squares (PDG) in figure 7. From a standard linear regression method we obtain the experimental and theoretical Regge trajectories for vector meson  $\rho$  belonging to the  $S$ -wave, so that:

$$m_{Exp}^2 = (1.363 \pm 0.092) n_r - (0.648 \pm 0.252), \quad (5.9)$$

$$m_{th}^2 = (1.357 \pm 0.213) n_r - (0.754 \pm 0.584). \quad (5.10)$$

Note that the Regge trajectory for the vector mesons belonging to the  $S$ -wave coming from our model, represented by Eq. (5.10), present a Regge slope in the range  $1.25 \pm 0.15$   $\text{GeV}^2$  which is close to the universal value  $1.1 \text{ GeV}^2$  [59, 62].

As a comment, if we follow the original motivation for the softwall model, it could be natural to suppose  $k_{sm}$  and  $k_{vm}$  related to the string tension for the flux tube that connects

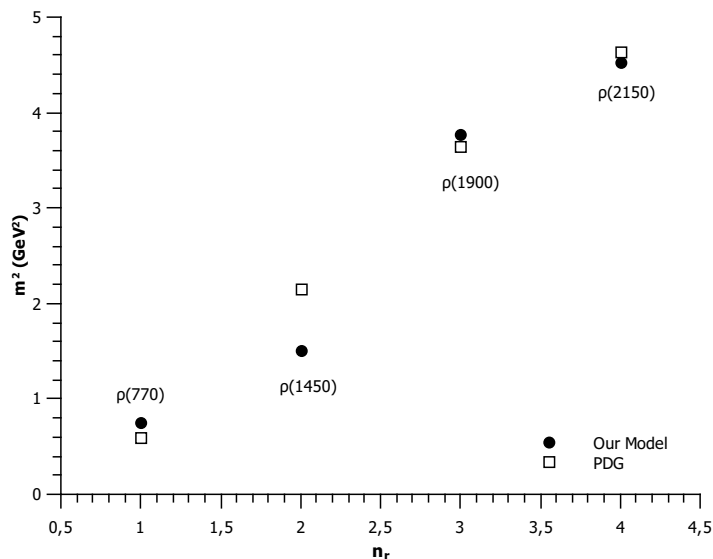


**Figure 7.** Vector mesons  $\rho$  belonging to  $S$ -wave (see the text) squared masses as a function of their spectroscopy radial excitation  $n_r$  obtained within the deformed  $AdS_5$  space approach (dots) and coming from PDG (squares).

the two quarks inside the meson. This information is contained in the confining part of the  $q\bar{q}$  potential, and it is, in principle, a spin independent term. Therefore, in the AdS/QCD models with dilatons in the action, the slope parameter should be universal for scalar and vector mesons, as it happens in the usual soft wall model [15, 42].

It is interesting to point out that  $k_{sm}$  and  $k_{vm}$  are related, namely  $3k_{sm} \approx k_{vm}$ . This quite interesting peculiarity possibly can be explained due to the fact that in the EOM for scalar mesons, Eq.(3.3), we performed the following substitution  $B(z) = -3A(z)$ . On the other hand, in the EOM for vector mesons, Eq.(5.3), we have used  $B(z) = -A(z)$ , and so, leading to  $k_{vm} \approx 3k_{sm}$ .

## 6 Hadronic spectra for baryons

Within the quark model constituent baryons are particles with semi integer spin formed by a bound state of three valence quarks. Of course, here, we are disregarding more complex states of baryons composed by three quarks added to any number of quark and antiquark pairs, as for instance, in pentaquark states ( $qqqq\bar{q}$ ). In this sense, one can use the following description for baryons, so that:

$$|qqq\rangle_A = |\text{color}\rangle_A \otimes |\text{space; spin-flavor}\rangle_S. \quad (6.1)$$

The three colors are represented by an  $SU(3)$  singlet, without dynamics and completely antisymmetric. The spatial wave function is related to  $O(6)$  and the spin-flavor wave function is related to the  $SU(6)$ . For a review in baryon physics one can see for instance

[63, 64]. Here, in this work we are interested in light baryons composed by  $u$  and  $d$  quarks with spin 1/2 and also with higher spins (3/2 and 5/2).

Within the holographic description of baryons are dual to the massive spinor fields in  $AdS_5$ . Then let us start our discussion from the free spinor field action without surface terms [65–68]:

$$S = \int_{AdS} d^5x \sqrt{g} \bar{\Psi} (\not{D} - m_5) \Psi. \quad (6.2)$$

One can note that we disregarded the hypersphere  $S^5$  since for our purposes the spinor field does not depend on these coordinates. Besides, in the action (6.2),  $g$  is the determinant of the metric of the deformed  $AdS_5$  space, given by (2.4).

Once we are dealing with fermions in a curved space, one needs to construct a local Lorentz frame or a vielbein. In order to clarify our notation, we will use  $a, b, c$  to denote indexes in flat space, and  $m, n, p, q$  to denote indexes in curved space (deformed  $AdS_5$  space). In addition, the Greek indexes  $\mu, \nu$  are defined in Minkowski space. Then, a useful choice is:

$$e_m^a = e^{A(z)} \delta_m^a, \quad e_a^m = e^{-A(z)} \delta_a^m e^{ma} = e^{-A(z)} \eta^{ma}, \quad \text{with} \quad m = 0, 1, 2, 3, 5. \quad (6.3)$$

The Levi-Civita connection is defined as:

$$\Gamma_{mn}^p = \frac{1}{2} g^{pq} (\partial_n g_{mq} + \partial_m g_{nq} - \partial_q g_{mn}), \quad \text{with} \quad g_{mn} = e^{2A(z)} \eta_{mn}. \quad (6.4)$$

The corresponding spin connection  $\omega_m^{\mu\nu}$ , is given by:

$$\omega_m^{ab} = e_n^a \partial_m e^{nb} + e_n^a e^{pb} \Gamma_{pm}^n. \quad (6.5)$$

Since only non-vanishing  $\Gamma_{mn}^p$  are:

$$\Gamma_{\mu\nu}^5 = A'(z) \eta_{\mu\nu}, \quad \Gamma_{55}^5 = -A'(z) \quad \text{and} \quad \Gamma_{\nu 5}^\mu = -A'(z) \delta_\nu^\mu, \quad (6.6)$$

we just have:

$$\omega_\mu^{5\nu} = -\omega_\mu^{\nu 5} = \partial_z A(z) \delta_\mu^\nu, \quad (6.7)$$

and all other components vanishing.

The equations of motion are easily derived from (6.2), so that:

$$(\not{D} - m_5) \Psi = 0 \quad \text{and} \quad \bar{\Psi} (-\overleftarrow{\not{D}} - m_5) = 0. \quad (6.8)$$

Now using (2.4), (6.3) and (6.7), one can write the operator  $\not{D}$  in (6.8), so that:

$$\not{D} \equiv g^{mn} e_n^a \gamma_a \left( \partial_m + \frac{1}{2} \omega_m^{bc} \Sigma_{bc} \right) = e^{-A(z)} \gamma^5 \partial_5 + e^{-A(z)} \gamma^\mu \partial_\mu + 2A'(z) \gamma^5, \quad (6.9)$$

where we used that  $\gamma_a = (\gamma_\mu, \gamma_5)$ ,  $\{\gamma_a, \gamma_b\} = 2\eta_{ab}$ , and  $\Sigma_{\mu 5} = \frac{1}{4} [\gamma_\mu, \gamma_5]$ . Here,  $\gamma_\mu$  are the usual Dirac's gamma matrices.

The first Dirac equation in (6.8) takes the following form:

$$\left( e^{-A(z)} \gamma^5 \partial_5 + e^{-A(z)} \gamma^\mu \partial_\mu + 2A'(z) \gamma^5 - m_5 \right) \Psi = 0, \quad (6.10)$$



where  $\partial_5 \equiv \partial_z$ ,  $z$  is the holographic coordinate in the AdS space and  $m_5$  is the fermion bulk mass. Considering a solution which can be decomposed into right- and left-handed chiral components, such as:

$$\Psi(x^\mu, z) = \left[ \frac{1 - \gamma^5}{2} f_L(z) + \frac{1 + \gamma^5}{2} f_R(z) \right] \Psi_{(4)}(x), \quad (6.11)$$

with  $\Psi_{(4)}(x)$  satisfying the Dirac equation  $(\not{D} - M)\Psi_{(4)}(x) = 0$  on the four-dimensional boundary space. The left and right modes also obey  $\gamma^5 f_{L/R} = \mp f_{L/R}$  and  $\gamma^\mu \partial_\mu f_R = m f_L$ .

Since the Kaluza-Klein modes are dual to the chirality spinors, one can expand  $\Psi_{L/R}$ , so that:

$$\Psi_{L/R}(x^\mu, z) = \sum_n f_{L/R}^n(x^\mu) \phi_{L/R}^n(z). \quad (6.12)$$

Using (6.12) with (6.11) in (6.10) one gets a set with two coupled equations, such as:

$$\left( \partial_z + 2A'(z) e^{A(z)} + m_5 e^{A(z)} \right) \phi_L^n(z) = +M_n \phi_R^n(z) \quad (6.13)$$

and

$$\left( \partial_z + 2A'(z) e^{A(z)} - m_5 e^{A(z)} \right) \phi_R^n(z) = -M_n \phi_L^n(z). \quad (6.14)$$

Decoupling Eqs.(6.13) and (6.14), and using the following changing of variables

$$\phi_{L/R}(z) = \psi(z) e^{-2e^{A(z)}}, \quad (6.15)$$

one gets a Schrödinger-like equation written for both right and left sectors, given by:

$$-\psi_{R/L}''(z) + \left[ m_5^2 e^{2A(z)} \pm m_5 e^{A(z)} A'(z) \right] \psi_{R/L}(z) = M_n^2 \psi_{R/L}(z), \quad (6.16)$$

where  $M_n$  in Eqs. (6.16) are the four-dimensional fermion masses.

### 6.1 Results for spin 1/2 baryons spectra

In this subsection we will deal with light baryons with spin  $S = 1/2$  formed by  $u$  and  $d$  quarks. In order to do this, let us consider the following operator on the boundary theory:

$$\mathcal{O}_B = q D_{\{\ell_1 \dots D_{\ell_i} q D_{\ell_{i+1}} \dots D_{\ell_m}\}} q; \quad \text{with} \quad \sum_{i=1} \ell_i = L, \quad (6.17)$$

where  $L$  is the orbital angular momentum. Here we are going to consider only the case  $L = 0$ .

From the AdS/CFT dictionary one has following relationship for the fermion bulk mass ( $m_5$ ) and its conformal dimension ( $\Delta$ ), so that:

$$|m_5| = \Delta - 2. \quad (6.18)$$

As each quark  $u$  or  $d$  contributes with  $\Delta = 3/2$ , then the baryon formed by three quarks has  $\Delta = 9/2$  and consequently  $m_5 = 5/2$ .

Now replacing  $m_5 = 5/2$  in the Schrödinger-like equation (6.16) and solving it numerically, with the warp factor constant  $k$  now identified by  $k_{1/2} = 0.205^2 \text{ GeV}^2$ , one gets the

	Baryons $N(1/2^+)$			
	$N$ baryon	$M_{\text{exp}}$ GeV [56]	$M_{\text{th}}$ GeV	$\%M$
$n = 1$	$N(939)$	$0.93949 \pm 0.00005$	0.98683	5.04
$n = 2$	$N(1440)$	1.360 to 1.380	1.264	7.76
$n = 3$	$N(1710)$	1.680 to 1.720	1.531	9.94
$n = 4$	$N(1880)$	1.820 to 1.900	1.791	3.70
$n = 5$	$N(2100)$	2.050 to 2.150	2.046	2.58
$n = 6$	$N(2300)$	$2.300^{+0.006}_{-0.005} \text{ } ^{+0.1}_{-0}$	2.296	0.19

**Table 5.** Masses of  $N(1/2^+)$  baryons. The column  $n = 1, 2, 3, \dots$  represents the holographic radial excitation. One should note that the ground state here is represented by  $n = 1$ . The column  $M_{\text{exp}}$  represents the experimental data coming from PDG [56]. The column  $M_{\text{th}}$  represents the masses of  $N(1/2^+)$  baryons with  $k_{1/2} = 0.205^2$  GeV<sup>2</sup> obtained within the deformed  $AdS_5$  space approach and using Eq.(6.16). The column  $\%M$  represents the error of  $M_{\text{th}}$  with respect to  $M_{\text{exp}}$ , accordingly to Eq. (4.3).

masses compatibles with the family of  $N$  baryon, with  $I(J^P) = 1/2(1/2^+)$ , as can be seen in table 5. Note that the error presented in last column of Table 5 ( $\%M$ ) was defined in Eq.(4.3). We also compute the total r.m.s error defined by Eq. (4.4). For table 5 one finds  $\delta_{rms} = 4.09\%$ .

From Table 5 we plotted a Chew-Frautschi plane here represented as  $n \times m^2$ , where  $n$  is holographic radial excitation and  $m^2$  is the squared  $N(1/2^+)$  baryon mass represented by the dots (our model) or squares (PDG) in figure 8. From a standard linear regression method we obtain the experimental and theoretical Regge trajectories for  $N(1/2^+)$  baryon, so that:

$$m_{Exp}^2 = (0.863 \pm 0.029) n + (0.114 \pm 0.111), \quad (6.19)$$

$$m_{th}^2 = (0.860 \pm 0.042) n - (0.081 \pm 0.164). \quad (6.20)$$

As was done for scalar and vector mesons one can resort to the baryonic spectroscopy and try to recognize which baryons among those listed in Table 5 belong to the same spectroscopy state. Following refs. [63, 64], one can see that the states  $N(939)$ ,  $N(1440)$ ,  $N(1710)$  and  $N(2100)$  belong to the state  $D_L \equiv (56, {}^2 8)_0$  with spectroscopy radial excitation  $n_r$ , corresponding to  $n_r = 1, 2, 3, 4$ , respectively, with orbital angular momentum  $L = 0$ . In this notation,  $D$  represents the 56-plet which can be broken into an octet with spin 1/2 ( ${}^2 8$ ) and a decuplet with spin 3/2 ( ${}^4 10$ ). For these mentioned states one can plot in a Chew-Frautschi plane here represented as  $n_r \times m^2$ , where  $n_r$  is the spectroscopy radial excitation and  $m^2$  is the squared  $N(1/2^+)$  baryon mass belonging to the  $(56, {}^2 8)_0$  state represented by the dots (our model) or squares (PDG) in figure 9. From a standard linear regression method we obtain the experimental and theoretical Regge trajectories for  $N(1/2^+)$  baryon in the  $(56, {}^2 8)_0$  state, so that:

$$m_{Exp}^2 = (1.160 \pm 0.090) n_r - (0.384 \pm 0.246), \quad (6.21)$$

$$m_{th}^2 = (1.038 \pm 0.204) n_r - (0.320 \pm 0.560). \quad (6.22)$$

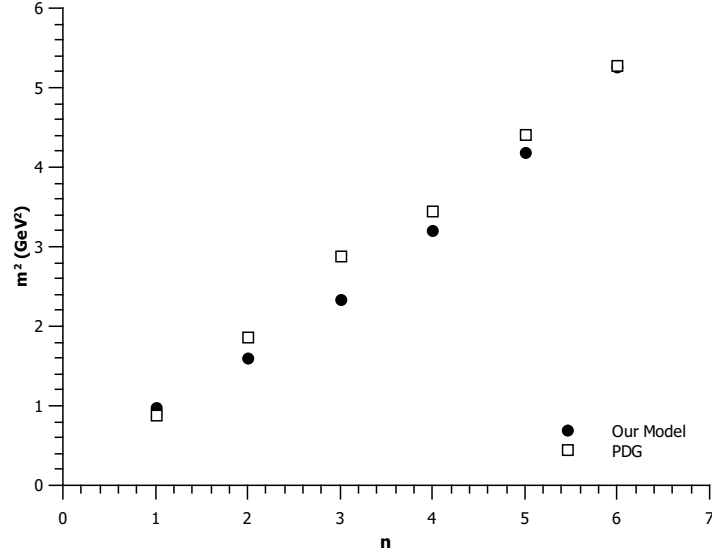


**Figure 8.**  $N(1/2^+)$  baryon family squared masses as a function of their holographic radial excitation obtained within the deformed  $AdS_5$  space approach (dots) and coming from PDG (squares), as presented in Table 5.

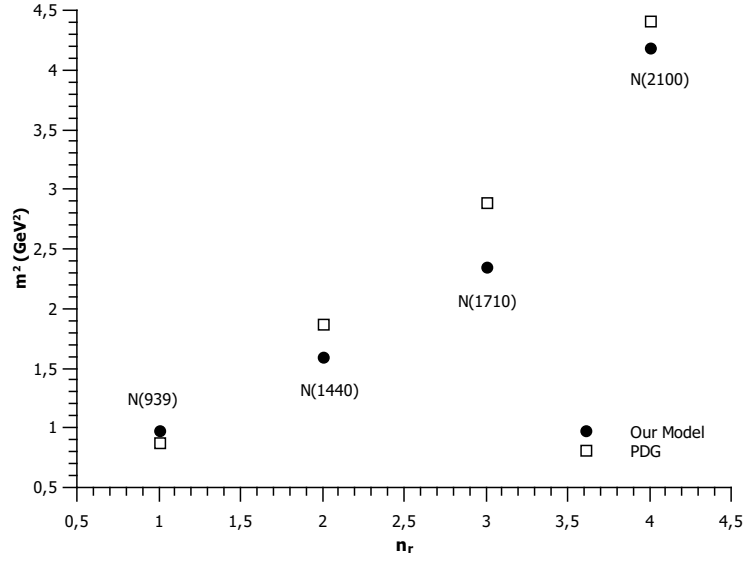


**Figure 9.**  $N(1/2^+)$  baryons belonging to the  $(56,^2 8)_0$  state squared masses as a function of their spectroscopy radial excitation  $n_r$  obtained within the deformed  $AdS_5$  space approach (dots) and coming from PDG (squares).

Note that the Regge trajectory for the  $N(1/2^+)$  baryon belonging to the same multiplet coming from our model, represented by Eq. (6.22), present a Regge slope in the range  $1.081 \pm 0.036 \text{ GeV}^2$  which is close to the universal value  $1.1 \text{ GeV}^2$  [69].

	Baryons $N(3/2^+)$			
	$N$ baryon	$M_{\text{exp}}$ GeV [56]	$M_{\text{th}}$ GeV	$\%M$
$n = 1$	$N(1720)$	1.660 to 1.690	1.326	23.05%
$n = 2$	$N(1900)$	1.900 to 1.940	1.606	12.27%
$n = 3$	$N(2040)$	$2.040^{+0.003}_{-0.004} \pm 0.025$	1.878	8.72%

**Table 6.** Masses of  $N(3/2^+)$  baryons. The column  $n = 1, 2, 3, \dots$  represents the holographic radial excitation. One should note that the ground state here is represented by  $n = 1$ . The column  $M_{\text{exp}}$  represents the experimental data coming from PDG [56]. The column  $M_{\text{th}}$  represents the masses of  $N(3/2^+)$  baryons with  $k_{3/2} = 0.205^2 \text{ GeV}^2$  obtained within the deformed  $AdS_5$  space approach and using Eq.(6.16). The column  $\%M$  represents the error of  $M_{\text{th}}$ , accordingly to Eq. (4.3).

## 6.2 Results for higher spin baryons spectra

Here we are interested in dealing with light baryons, with the same structure as in previous section, and higher spin, meaning  $S = 3/2$  or  $S = 5/2$ , for example. To do this we will use the same approach for higher spin glueball as done in subsection 3.1. To get the spectrum for spin 3/2 baryons we will insert symmetrised covariant derivatives in the operator  $\mathcal{O}_B$  given by (6.17) then the conformal dimensions related to the spin 3/2 baryons is now  $\Delta_{3/2} = 11/2$ , with  $m_5 = 7/2$ . Solving Eq. (6.16) with the warp factor constant  $k$  now given by  $k_{3/2} = 0.205^2 \text{ GeV}^2$ , one gets the masses compatibles with the family of  $N$  baryon, with  $I(J^P) = 1/2(3/2^+)$ , as can be seen in table 6. Note that the error presented in last column of table 6 ( $\%M$ ) was defined in Eq.(4.3). We also compute the total r.m.s error defined by Eq. (4.4). For table 7 one finds  $\delta_{rms} = 9.00\%$ .

Observing the column ( $\%M$ ) in Table 6 one can see that errors between  $M_{\text{exp}}$  and  $M_{\text{th}}$  are too high, especially for  $n = 1$  and  $n = 2$  states. A possible reinterpretation would be a missing state that represents the ground state for  $N(3/2^+)$  baryons family. Taking into account this assumption, regarding to a possible missing state, one can reinterpret the Table 6 as done in Table 7, where in the first line we present a possible baryon prediction obtained within this deformed AdS model. Note that the error presented in last column of table 7 ( $\%M$ ) was defined in Eq.(4.3). We also compute the total r.m.s error defined by Eq. (4.4). For table 7 one finds  $\delta_{rms} = 2.13\%$ . Of course we have excluded our prediction of the errors calculation. Note that the errors in Table 6 are smaller than in Table 7.

From Table 7 we plotted a Chew-Frautschi plane here represented as  $n \times m^2$ , where  $n$  is holographic radial excitation and  $m^2$  is the squared  $N(3/2^+)$  baryon mass represented by the dots (our model), by the triangle (our model prediction) or squares (PDG) in figure 10. From a standard linear regression method we obtain the experimental and theoretical Regge trajectories for  $N(3/2^+)$  baryons, so that:

$$m_{Exp}^2 = (0.678 \pm 0.117) n + (1.517 \pm 0.364), \quad (6.23)$$

$$m_{th}^2 = (1.021 \pm 0.017) n + (0.501 \pm 0.047). \quad (6.24)$$

For the linear fit in Eq.(6.24) we took into account our predicted state.

	Baryons $N(3/2^+)$			
	$N$ baryon	$M_{\text{exp}}$ GeV [56]	$M_{\text{th}}$ GeV	$\%M$
$n = 1$			1.326	
$n = 2$	$N(1720)$	1.660 to 1.690	1.606	4.14
$n = 3$	$N(1900)$	1.900 to 1.940	1.878	2.19
$n = 4$	$N(2040)$	$2.040^{+0.003}_{-0.004} \pm 0.025$	2.144	5.09

**Table 7.** Masses of  $N(3/2^+)$  baryons. The column  $n = 1, 2, 3, \dots$  represents the holographic radial excitation. One should note that the ground state here is represented by  $n = 1$ . The column  $M_{\text{exp}}$  represents the experimental data coming from PDG [56]. The column  $M_{\text{th}}$  represents the masses of  $N(3/2^+)$  baryons with  $k_{3/2} = 0.205^2 \text{ GeV}^2$  obtained within the deformed  $AdS_5$  space approach and using Eq.(6.16). The column  $\%M$  represents the error of  $M_{\text{th}}$  with respect to  $M_{\text{exp}}$ , accordingly to Eq. (4.3). We presented in the first line a possible baryon prediction within our model.

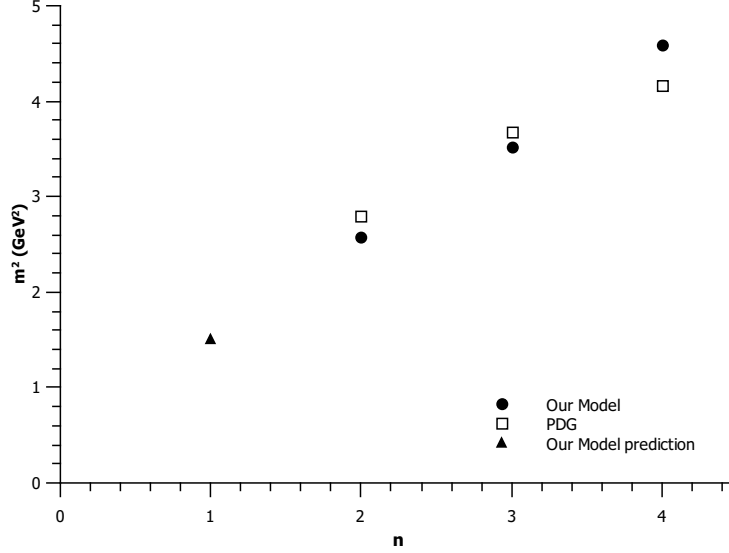


**Figure 10.**  $N(3/2^+)$  baryon family squared masses as a function of their holographic radial excitation obtained within the deformed  $AdS_5$  space approach (dots), our model prediction (triangle) and coming from PDG (squares), as presented in Table 7.

Note that the Regge trajectory for the  $N(3/2^+)$  baryon family coming from our model, represented by Eq. (6.24), present a Regge slope in the range  $1.081 \pm 0.036 \text{ GeV}^2$  which is close to the universal value  $1.1 \text{ GeV}^2$  [69].

At this point we are interested to deal with baryons with spin  $5/2$ . To do this, let us, once again, insert one more symmetrised covariant derivative in the operator  $\mathcal{O}_B$  given by (6.17). Then, one has the conformal dimension, now given by  $\Delta_{5/2} = 13/2$ , which provides  $m_5 = 9/2$ . Solving Eq. (6.16) with the warp factor constant  $k$  now given by  $k_{5/2} = 0.190^2 \text{ GeV}^2$ , one gets the masses compatible with the family of  $N$  baryons, with  $I(J^P) = 1/2(5/2^+)$ , as can be seen in table 8. Note that the error presented in the last

	Baryons $N(5/2^+)$			
	$N$ baryon	$M_{\text{exp}}$ GeV [56]	$M_{\text{th}}$ GeV	$\%M$
$n = 1$	$N(1680)$	1.665 to 1.680	1.542	7.78
$n = 2$	$N(1860)$	$1.830^{+120}_{-60}$	1.804	1.44
$n = 3$	$N(2000)$	$2.090 \pm 120$	2.059	1.49

**Table 8.** Masses of  $N(5/2^+)$  baryons. The column  $n = 1, 2, 3, \dots$  represents the holographic radial excitation. One should note that the ground state here is represented by  $n = 1$ . The column  $M_{\text{exp}}$  represents the experimental data coming from PDG [56]. The column  $M_{\text{th}}$  represents the masses of  $N(5/2^+)$  baryons with  $k_{5/2} = 0.190^2 \text{ GeV}^2$  obtained within the deformed  $AdS_5$  space approach and using Eq.(6.16). The column  $\%M$  represents the error of  $M_{\text{th}}$  with respect to  $M_{\text{exp}}$ , accordingly to Eq. (4.3).

column of table 8 ( $\%M$ ) was defined in Eq. (4.3). We also compute the total r.m.s error defined by Eq. (4.4). For table 8 one finds  $\delta_{rms} = 2.76\%$ .

From Table 8 we plotted a Chew-Frautschi plane as  $n \times m^2$ , where  $n$  is holographic radial excitation and  $m^2$  is the squared  $N(5/2^+)$  baryon mass represented by the dots (our model) or squares (PDG) in figure 11. From a standard linear regression method we obtain the experimental and theoretical Regge trajectories for  $N(5/2^+)$  baryons, so that:

$$m_{Exp}^2 = (0.785 \pm 0.135) n + (1.934 \pm 0.291), \quad (6.25)$$

$$m_{th}^2 = (0.931 \pm 0.031) n + (1.429 \pm 0.068). \quad (6.26)$$

Note that the Regge trajectory for the  $N(5/2^+)$  baryon family coming from our model, represented by Eq. (6.26), present a Regge slope near the range  $1.081 \pm 0.036 \text{ GeV}^2$  which is close to the universal value  $1.1 \text{ GeV}^2$  [69].

At this point it is worth to mention that the numeric values of the warp factor constant  $k$  for the baryons studied here are approximately independent of their spin, meaning that  $k_{1/2} = k_{3/2} \approx k_{5/2}$ .

## 7 Summary and conclusions

In this section we will summarize our results, and present our conclusions and last comments.

Here in this work we have studied the hadronic spectra based on the holographic model within a deformed  $AdS_5$  space metric meaning that the warp factor is  $A(z) = -\log(z) + kz^2/2$  instead of  $A(z) = -\log(z)$  as in the pure AdS space. This deformation implies that there is no dilaton field in the action as in the original softwall model.

The main achievement of this work is to provide a model which can accommodate satisfactorily the spectra for even and odd glueballs, scalar ( $0^+(0^{++})$ ) and vector mesons ( $1^+(1^{--})$ ),  $N$  baryons with spin  $1/2$ ,  $3/2$  and  $5/2$  using the same holographic approach. This means that the masses of these mentioned particles, computed using our model, and the derived Regge trajectories are in agreement with the literature.

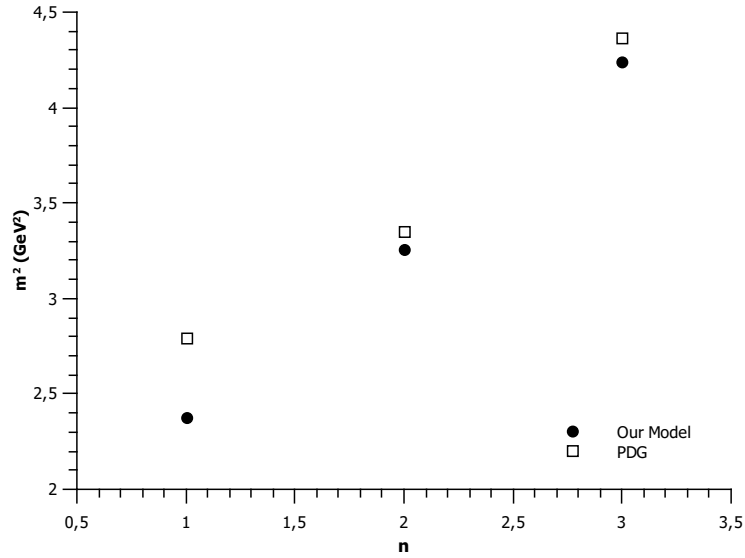


**Figure 11.**  $N(5/2^+)$  baryon family squared masses as a function of their holographic radial excitation obtained within the deformed  $AdS_5$  space approach (dots) and coming from PDG (squares), as presented in Table 8.

For the even and odd glueball cases, our model seems to work providing good masses, as one can see in Tables 1 and 2 if compared with other approaches (for a summary with even and odd spin glueball masses from lattice and other models, see for instance refs. [51] [44]). The computed masses for higher even and odd spin glueballs were placed in a Chew-Frautschi plane  $m^2 \times J$ . We derived the Regge trajectories related to the pomeron and the odderon in agreement with the literature.

Our model seems to work for scalar mesons providing good masses for the  $f_0$  ( $0^+(0^{++})$ ), as one can see in table 3, if one compares with the data coming from PDG [56]. The obtained Regge trajectory coming from  $m^2 \times n$  is compatible with the one coming from the holographic softwall model [57, 58]. Using the spectroscopy data for the scalar mesons we could split them into two sets. The first one only contains  $n\bar{n} = 1/\sqrt{2}(u\bar{u} + d\bar{d})$  while the second one only contains  $s\bar{s}$ . For these sets we derived Regge trajectories in  $m^2 \times n_r$  which is compatible with the literature [59, 62].

For the vector meson  $\rho(1^+(1^{--}))$  our model provided good masses as shown in table 4 compared with PDG. The obtained Regge trajectory coming from  $m^2 \times n$  is compatible with the one coming from the holographic softwall model [57, 58]. Using the spectroscopy data for the vector mesons we selected the  $S$ -wave states and derived their Regge trajectory in  $m^2 \times n_r$  which is agreement with the literature [59, 62].

Our model also provides good masses for  $N(1/2^+)$  baryon, as can be seen in table 5, compared with PDG. In this case we also have used the baryonic spectroscopic data to select states in the same multiplet, just varying their radial excitation. From these states we derived the Regge trajectory compatible with the literature [69].

For the  $N(3/2^+)$  baryon we found not so good results for the masses as can be seen in table 6. These results could be improved if we introduce a hypothetical baryonic state in order to occupy the ground state (table 7). Using this assumption the errors decrease and the derived Regge trajectory is compatible with the literature [69].

Finally, for the  $N(5/2^+)$  baryon our model provide good masses as can be seen in table 8, if compared with PDG and the Regge trajectory is in a reasonable agreement with the [69].

It is important to note that in our model the warp factor is the same for all particles studied here, up to the constant  $k$ . This is in contrast with [25] which has different warp factors for each kind of particle. In our case, for even and odd glueballs the value of  $k$  is the same,  $k_{gbe} = k_{gbo} = 0.31^2 \text{ GeV}^2$ . For scalar and vector mesons we found that  $k_{vm} \approx 3k_{sm}$ , as discussed at the end of subsection 5.1. For the baryonic case, we found  $k_{1/2} = k_{3/2} \approx k_{5/2}$ .

The Regge trajectories presented in this work related to hadronic spectroscopy for scalar mesons (4.8), (4.10), vector mesons (5.10), and baryons (6.22), (6.24), (6.26) points towards a universal Regge slope around  $1.1 \text{ GeV}^2$  in accordance with the literature [59, 62, 69, 70].

## Acknowledgments

E.F.C. would like to thanks Carlos Alfonso Ballon Bayona for useful conversations. H.B-F. would like to thank Conselho Nacional de Desenvolvimento Científico e Tecnológico (CNPq) and Coordenação de Aperfeiçoamento de Pessoal de Nível Superior (Capes) (Brazilian Agencies). A. V. and M. A. M. C. would like to thank the financial support given by FONDECYT (Chile) under Grants No. 1180753 and No. 3180592 respectively. D.L. is supported by the National Natural Science Foundation of China (No.11805084) and the PhD Start-up Fund of Natural Science Foundation of Guangdong Province (No.2018030310457).

## References

- [1] J. M. Maldacena, “The Large N limit of superconformal field theories and supergravity,” Adv. Theor. Math. Phys. **2**, 231 (1998) [hep-th/9711200].
- [2] S. S. Gubser, I. R. Klebanov and A. M. Polyakov, “Gauge theory correlators from noncritical string theory,” Phys. Lett. B **428**, 105 (1998) [hep-th/9802109].
- [3] E. Witten, “Anti-de Sitter space and holography,” Adv. Theor. Math. Phys. **2**, 253 (1998) [hep-th/9802150].
- [4] E. Witten, “Anti-de Sitter space, thermal phase transition, and confinement in gauge theories,” Adv. Theor. Math. Phys. **2**, 505 (1998) [hep-th/9803131].
- [5] O. Aharony, S. S. Gubser, J. M. Maldacena, H. Ooguri and Y. Oz, “Large N field theories, string theory and gravity,” Phys. Rept. **323**, 183 (2000) [hep-th/9905111].
- [6] J. Polchinski and M. J. Strassler, “Hard scattering and gauge / string duality,” Phys. Rev. Lett. **88**, 031601 (2002) [hep-th/0109174].
- [7] H. Boschi-Filho and N. R. F. Braga, “Gauge / string duality and scalar glueball mass ratios,” JHEP **0305**, 009 (2003) [hep-th/0212207].



- [8] H. Boschi-Filho and N. R. F. Braga, “QCD / string holographic mapping and glueball mass spectrum,” *Eur. Phys. J. C* **32**, 529 (2004) [hep-th/0209080].
- [9] J. Erlich, E. Katz, D. T. Son and M. A. Stephanov, “QCD and a holographic model of hadrons,” *Phys. Rev. Lett.* **95**, 261602 (2005) [hep-ph/0501128].
- [10] L. Da Rold and A. Pomarol, “Chiral symmetry breaking from five dimensional spaces,” *Nucl. Phys. B* **721**, 79 (2005) [hep-ph/0501218].
- [11] G. F. de Teramond and S. J. Brodsky, “Hadronic spectrum of a holographic dual of QCD,” *Phys. Rev. Lett.* **94**, 201601 (2005) [hep-th/0501022].
- [12] L. Da Rold and A. Pomarol, “The Scalar and pseudoscalar sector in a five-dimensional approach to chiral symmetry breaking,” *JHEP* **0601**, 157 (2006) [hep-ph/0510268].
- [13] A. Pomarol and A. Wulzer, “Baryon Physics in Holographic QCD,” *Nucl. Phys. B* **809**, 347 (2009) [arXiv:0807.0316 [hep-ph]].
- [14] Z. Li and B. Q. Ma, “Baryon spectrum in a finite-temperature AdS/QCD model,” *Phys. Rev. D* **89**, no. 1, 015014 (2014) doi:10.1103/PhysRevD.89.015014 [arXiv:1312.3451 [hep-ph]].
- [15] A. Karch, E. Katz, D. T. Son and M. A. Stephanov, “Linear confinement and AdS/QCD,” *Phys. Rev. D* **74**, 015005 (2006) [hep-ph/0602229].
- [16] A. Vega and I. Schmidt, “Hadrons in AdS/QCD correspondence,” *Phys. Rev. D* **79**, 055003 (2009) [arXiv:0811.4638 [hep-ph]].
- [17] T. Branz, T. Gutsche, V. E. Lyubovitskij, I. Schmidt and A. Vega, “Light and heavy mesons in a soft-wall holographic approach,” *Phys. Rev. D* **82**, 074022 (2010) [arXiv:1008.0268 [hep-ph]].
- [18] T. Gutsche, V. E. Lyubovitskij, I. Schmidt and A. Vega, “Dilaton in a soft-wall holographic approach to mesons and baryons,” *Phys. Rev. D* **85**, 076003 (2012) [arXiv:1108.0346 [hep-ph]].
- [19] S. S. Afonin, “Generalized Soft Wall Model,” *Phys. Lett. B* **719**, 399 (2013) [arXiv:1210.5210 [hep-ph]].
- [20] Z. Fang, D. Li and Y. L. Wu, “IR-improved Soft-wall AdS/QCD Model for Baryons,” *Phys. Lett. B* **754**, 343 (2016) [arXiv:1602.00379 [hep-ph]].
- [21] S. Cortés, M. Á. Martín Contreras and J. R. Roldán, *Phys. Rev. D* **96**, no. 10, 106002 (2017) [arXiv:1706.09502 [hep-ph]].
- [22] M. Á. Martín Contreras, A. Vega and S. Cortés, “Light Pseudoscalar and Axial Spectroscopy using AdS/QCD Modified Soft Wall Model,” arXiv:1811.10731 [hep-ph].
- [23] S. S. Afonin and A. D. Katanaeva, “Glueballs and deconfinement temperature in AdS/QCD,” *Phys. Rev. D* **98**, no. 11, 114027 (2018) [arXiv:1809.07730 [hep-ph]].
- [24] T. Gutsche, V. E. Lyubovitskij, I. Schmidt and A. Y. Trifonov, “Mesons in a soft-wall AdS-Schwarzschild approach at low temperature,” arXiv:1902.01312 [hep-ph].
- [25] H. Forkel, M. Beyer and T. Frederico, “Linear square-mass trajectories of radially and orbitally excited hadrons in holographic QCD,” *JHEP* **0707**, 077 (2007) [arXiv:0705.1857 [hep-ph]].
- [26] O. Andreev and V. I. Zakharov, “Heavy-quark potentials and AdS/QCD,” *Phys. Rev. D* **74**, 025023 (2006) [hep-ph/0604204].

- [27] C. D. White, “The Cornell potential from general geometries in AdS / QCD,” *Phys. Lett. B* **652**, 79 (2007) [hep-ph/0701157].
- [28] R. C. L. Bruni, E. Folco Capossoli and H. Boschi-Filho, “Quark-antiquark potential from a deformed AdS/QCD,” *Adv. High Energy Phys.* **2019**, 1901659 (2019) [arXiv:1806.05720 [hep-th]].
- [29] M. Rinaldi and V. Vento, *Eur. Phys. J. A* **54**, 151 (2018) doi:10.1140/epja/i2018-12600-9 [arXiv:1710.09225 [hep-ph]].
- [30] S. Dobbs, A. Tomaradze, T. Xiao and K. K. Seth, “Comprehensive Study of the Radiative Decays of  $J/\psi$  and  $\psi(2S)$  to Pseudoscalar Meson Pairs, and Search for Glueballs,” *Phys. Rev. D* **91**, no. 5, 052006 (2015) [arXiv:1502.01686 [hep-ex]].
- [31] H. Fritzsch and M. Gell-Mann, “Current algebra: Quarks and what else?,” *eConf C* **720906V2**, 135 (1972) [hep-ph/0208010].
- [32] C. Augier *et al.* [UA4/2 Collaboration], “A Precise measurement of the real part of the elastic scattering amplitude at the S anti-p p S,” *Phys. Lett. B* **316**, 448 (1993).
- [33] R. Avila, P. Gauron and B. Nicolescu, “How can the Odderon be detected at RHIC and LHC,” *Eur. Phys. J. C* **49**, 581 (2007) [hep-ph/0607089].
- [34] M. Ablikim *et al.* [BES Collaboration], “Partial wave analyses of  $J/\psi \rightarrow \gamma \pi^+ \pi^-$  and  $\gamma \pi^0 \pi^0$ ,” *Phys. Lett. B* **642**, 441 (2006) [hep-ex/0603048].
- [35] J. Z. Bai *et al.* [BES Collaboration], “Partial wave analyses of  $J/\psi \rightarrow \gamma K^+ K^-$  and  $\gamma K_0(S) K_0(S)$ ,” *Phys. Rev. D* **68**, 052003 (2003) [hep-ex/0307058].
- [36] C. J. Morningstar and M. J. Peardon, “The Glueball spectrum from an anisotropic lattice study,” *Phys. Rev. D* **60**, 034509 (1999) [hep-lat/9901004].
- [37] H. B. Meyer and M. J. Teper, “Glueball Regge trajectories and the pomeron: A Lattice study,” *Phys. Lett. B* **605**, 344 (2005) [hep-ph/0409183].
- [38] Y. Chen, A. Alexandru, S. J. Dong, T. Draper, I. Horvath, F. X. Lee, K. F. Liu and N. Mathur *et al.*, “Glueball spectrum and matrix elements on anisotropic lattices,” *Phys. Rev. D* **73**, 014516 (2006) [hep-lat/0510074].
- [39] B. Lucini and M. Teper, “SU(N) gauge theories in four-dimensions: Exploring the approach to  $N = \infty$ ,” *JHEP* **0106**, 050 (2001) [hep-lat/0103027].
- [40] A. P. Szczepaniak and E. S. Swanson, “The Low lying glueball spectrum,” *Phys. Lett. B* **577**, 61 (2003) [hep-ph/0308268].
- [41] V. Mathieu, F. Buisseret and C. Semay, “Gluons in glueballs: Spin or helicity?,” *Phys. Rev. D* **77**, 114022 (2008) [arXiv:0802.0088 [hep-ph]].
- [42] P. Colangelo, F. De Fazio, F. Jugeau and S. Nicotri, “On the light glueball spectrum in a holographic description of QCD,” *Phys. Lett. B* **652** (2007) 73 [hep-ph/0703316].
- [43] H. Boschi-Filho, N. R. F. Braga and H. L. Carrion, “Glueball Regge trajectories from gauge/string duality and the Pomeron,” *Phys. Rev. D* **73**, 047901 (2006) [hep-th/0507063].
- [44] E. F. Capossoli and H. Boschi-Filho, “Odd spin glueball masses and the Odderon Regge trajectories from the holographic hardwall model,” *Phys. Rev. D* **88**, no. 2, 026010 (2013) [arXiv:1301.4457 [hep-th]].

- [45] D. M. Rodrigues, E. Folco Capossoli and H. Boschi-Filho, “Twist Two Operator Approach for Even Spin Glueball Masses and Pomeron Regge Trajectory from the Hardwall Model,” *Phys. Rev. D* **95**, no. 7, 076011 (2017) [arXiv:1611.03820 [hep-th]].
- [46] H. Boschi-Filho, N. R. F. Braga, F. Jugeau and M. A. C. Torres, “Anomalous dimensions and scalar glueball spectroscopy in AdS/QCD,” *Eur. Phys. J. C* **73**, 2540 (2013) [arXiv:1208.2291 [hep-th]].
- [47] D. Li and M. Huang, “Dynamical holographic QCD model for glueball and light meson spectra,” *JHEP* **1311**, 088 (2013) [arXiv:1303.6929 [hep-ph]].
- [48] E. Folco Capossoli and H. Boschi-Filho, “Glueball spectra and Regge trajectories from a modified holographic softwall model,” *Phys. Lett. B* **753**, 419 (2016) [arXiv:1510.03372 [hep-ph]].
- [49] E. Folco Capossoli, D. Li and H. Boschi-Filho, “Pomeron and Odderon Regge Trajectories from a Dynamical Holographic Model,” *Phys. Lett. B* **760**, 101 (2016) [arXiv:1601.05114 [hep-ph]].
- [50] E. Folco Capossoli, D. Li and H. Boschi-Filho, “Dynamical corrections to the anomalous holographic soft-wall model: the pomeron and the odderon,” *Eur. Phys. J. C* **76**, no. 6, 320 (2016) [arXiv:1604.01647 [hep-ph]].
- [51] D. M. Rodrigues, E. Folco Capossoli and H. Boschi-Filho, “Scalar and higher even spin glueball masses from an anomalous modified holographic model,” *EPL* **122**, no. 2, 21001 (2018) [arXiv:1611.09817 [hep-ph]].
- [52] A. Donnachie and P. V. Landshoff, “Dynamics of Elastic Scattering,” *Nucl. Phys. B* **267**, 690 (1986).
- [53] S. Donnachie, H. G. Dosch, O. Nachtmann and P. Landshoff, “Pomeron physics and QCD,” *Camb. Monogr. Part. Phys. Nucl. Phys. Cosmol.* **19**, 1 (2002).
- [54] F. J. Llanes-Estrada, P. Bicudo and S. R. Cotanch, “Oddballs and a low odderon intercept,” *Phys. Rev. Lett.* **96**, 081601 (2006) [hep-ph/0507205].
- [55] S. Godfrey and J. Napolitano, “Light meson spectroscopy,” *Rev. Mod. Phys.* **71**, 1411 (1999) [hep-ph/9811410].
- [56] M. Tanabashi *et al.* [Particle Data Group], “Review of Particle Physics,” *Phys. Rev. D* **98**, no. 3, 030001 (2018).
- [57] T. Gherghetta, J. I. Kapusta and T. M. Kelley, “Chiral symmetry breaking in the soft-wall AdS/QCD model,” *Phys. Rev. D* **79**, 076003 (2009) [arXiv:0902.1998 [hep-ph]].
- [58] T. M. Kelley, “The Dynamics and Thermodynamics of Soft-Wall AdS/QCD,” arXiv:1108.0653 [hep-ph].
- [59] A. V. Anisovich, V. V. Anisovich and A. V. Sarantsev, “Systematics of  $q$  anti- $q$  states in the  $(n, M^{**2})$  and  $(J, M^{**2})$  planes,” *Phys. Rev. D* **62**, 051502 (2000) [hep-ph/0003113].
- [60] D. Ebert, R. N. Faustov and V. O. Galkin, “Mass spectra and Regge trajectories of light mesons in the relativistic quark model,” *Phys. Rev. D* **79**, 114029 (2009) [arXiv:0903.5183 [hep-ph]].
- [61] J. K. Chen, “Concavity of the meson Regge trajectories,” *Phys. Lett. B* **786**, 477 (2018) [arXiv:1807.11003 [hep-ph]].

- [62] F. Iachello, N. C. Mukhopadhyay and L. Zhang, “Spectrum generating algebra for string like mesons. 1. Mass formula for  $q$  anti- $q$  mesons,” *Phys. Rev. D* **44**, 898 (1991).
- [63] E. Klempt and J. M. Richard, “Baryon spectroscopy,” *Rev. Mod. Phys.* **82**, 1095 (2010) [arXiv:0901.2055 [hep-ph]].
- [64] E. Klempt, “Baryon resonances and strong QCD,” nucl-ex/0203002.
- [65] M. Henningson and K. Sfetsos, “Spinors and the AdS / CFT correspondence,” *Phys. Lett. B* **431**, 63 (1998) [hep-th/9803251].
- [66] W. Mueck and K. S. Viswanathan, “Conformal field theory correlators from classical field theory on anti-de Sitter space. 2. Vector and spinor fields,” *Phys. Rev. D* **58**, 106006 (1998) [hep-th/9805145].
- [67] Z. Abidin and C. E. Carlson, “Nucleon electromagnetic and gravitational form factors from holography,” *Phys. Rev. D* **79**, 115003 (2009) [arXiv:0903.4818 [hep-ph]].
- [68] J. H. Gao and Z. G. Mou, “Polarized Deep Inelastic Scattering Off the Neutron From Gauge/String Duality,” *Phys. Rev. D* **81**, 096006 (2010) [arXiv:1003.3066 [hep-ph]].
- [69] E. Klempt, “A Mass formula for baryon resonances,” *Phys. Rev. C* **66**, 058201 (2002) [hep-ex/0206012].
- [70] D. V. Bugg, “Four sorts of meson,” *Phys. Rept.* **397**, 257 (2004) [hep-ex/0412045].